

**IMPEDANCE MEASUREMENTS OF STAINLESS DIFFERENT HEAT TREATED STEELS IN THE ACTIVE – PASSIVE REGION****Mojca Slemnik, Valter Doleček, and Miran Gaberšček\****Faculty of Chemistry and Chemical Engineering, Smetanova 17, 2000 Maribor, Slovenia**\*National Institute of Chemistry, Hajdrihova 19, 61115 Ljubljana, Slovenia**Received 25-09-2002***Abstract**

The behaviour of differently heat-treated X20Cr13 steels in 0.1 M H<sub>2</sub>SO<sub>4</sub> was studied using the classical potentiodynamic method and electrochemical impedance spectroscopy. On the base of the potentiodynamic curve the constant potentials have been chosen at which the impedance spectra were recorded: at the active peak, the potential next to the active peak and in the active - passive region. All impedance spectra show typical shapes: the high frequency portions have typical semicircular shapes of complex plane plots, whereas at low frequencies the plots deviate into semicircles running in opposite direction and yielding the so-called negative resistance as the frequency approaches 0 Hz. These spectra are interpreted in terms of a model by R.D. Armstrong describing, in a general way, the electrochemical reaction at interfaces with adsorbed intermediates.<sup>10</sup> Applying the model to the measured impedance spectra, we have been able to distinguish between the cases in which the observed charge transfer resistance is solely determined by nature of metal surface and the cases in which, beyond this inherent metal property, the charge transfer is determined by the degree of surface coverage with adsorbed intermediates. For example, while the oil-quenched X20Cr13 steel shows the lowest inherent charge transfer resistance of bare surface, the air-quenched sample exhibits the largest resistance due to surface passivation by intermediates. All results of impedance analysis are well-correlated to the measured potentiodynamic curves.

**Introduction**

Potentiodynamic polarization techniques permit the measurement of polarization behaviour by continuously scanning the potential while monitoring the current response. In the case of passivating systems, these techniques give useful information about the potential regions which correspond to the active and passive state and, in particular, about the active-passive transition region. However, this information is rather qualitative. It is not possible to discern between various reactions steps, such as adsorption and charge transfer reaction at the passivating interface. Hence, the corresponding quantitative parameters, e.g. charge transfer resistance, adsorption rate constant or adsorption capacity etc., are also not obtainable by these techniques. By contrast, such information can be gained using the electrochemical impedance spectroscopy (EIS).

EIS is a well-established technique for investigating electrochemical and corrosion systems.<sup>1-6</sup> An ac signal is applied to an electrode, here a corroding material, and the response is measured. Usually a small voltage signal is applied and the resulting current measured. The measuring equipment processes the current – time and the voltage – time measurements to provide the impedance at different frequencies, the impedance spectrum.<sup>7</sup>

In our former work, stainless steel X20Cr13 was exposed to various heat treatments: quenched on air, quenched in oil and quenched in oil and tempered. After the passivation, the measurements of electrochemical noise<sup>8</sup> and the impedance spectra<sup>9</sup> on the passive layers have been made with the purpose to determine the influence of the heat treatments on corrosion resistance of steels at the passivation potential. The values of passive layers resistance,  $R_{pl}$ , and interfacial capacitance,  $C_i$ , were determined.<sup>9</sup> However; the information was limited to the high and intermediate frequency regimes, while the low-frequency part of EIS spectra was considered only qualitatively.

In the present work we broaden the previous work by interpreting the EIS spectra measured in the active-passive transition in terms of a quantitative model developed by R.D. Armstrong in 1972.<sup>10</sup> In short, the model assumes that the active -passive transition occurs due to adsorbed species on a metal surface which block the charge transfer process. The adsorption of species is potential-dependent and is increased as the potential increases. This results in a pronounced increase of charge transfer resistance because charge transfer can only occur at spots on the metal surface where no species have been adsorbed.

During the measurement of impedance spectra, two types of processes occur (Fig.1): a) at high frequencies the adsorption process is essentially »frozen in«, and mainly the charge transfer is detected (the high-frequency arc A is observed in the complex plane); b) The low-frequency response is dominated by the adsorption/passivation process (arc B is observed). Note, however, that the parameters pertaining to the charge transfer reaction and adsorption/passivation processes are not clearly separated, i.e., they cannot be mapped directly into the two arcs observed. For example, although arc A in Fig.1 is dominated by the charge transfer reaction, the size of the arc is not directly related to the charge transfer resistance - in fact, as we will see

later, charge transfer resistance splits to several contributions in this model. We emphasize this issue because there is a general tendency in the field of EIS that the authors ascribe individual processes to individual arcs.

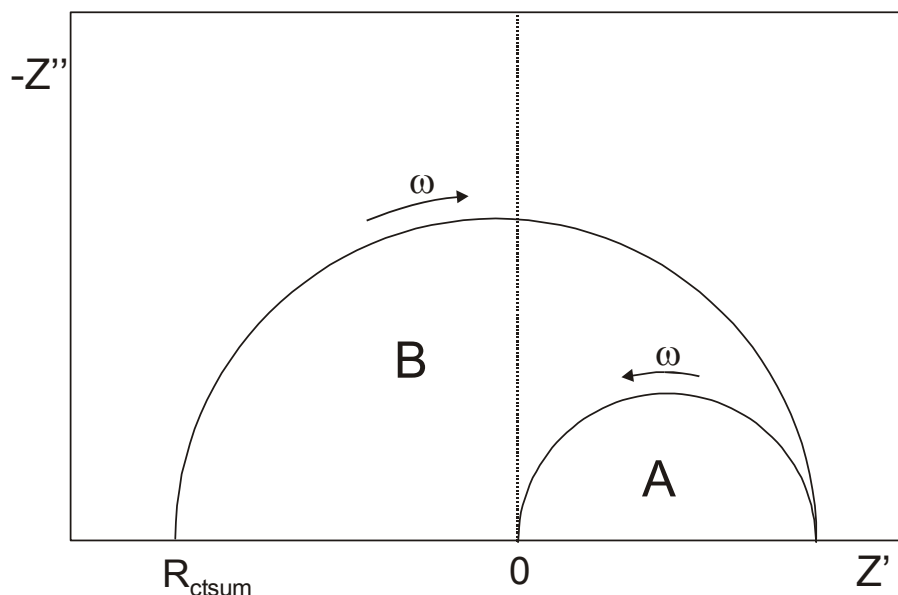


**Figure 1.** Typical shape of impedance response resulting from a model by R.D. Armstrong<sup>10</sup> presented in complex plane. A: high-frequency arc, B: low-frequency arc.  $R_{ctsum}$  is defined by Eq. (1),  $\omega$ : angular frequency of excitation signal.

The aim of the present work was to determine the change of charge transfer resistance when moving from active to passive region for three types of heat treatment on stainless steels. It is reasonable to assume that the larger this change the more effective is the passivation process. In this way, we should be able to get a quantitative measure which would tell us which of the selected heat treatment of steel is passivated most effectively.

#### Theoretical predictions of the adsorption-charge transfer reaction model

The model of R.D. Armstrong<sup>10</sup> contains 5 parameters, i.e., charge transfer resistance at »frozen in« adsorption,  $R_{ct\infty}$ , charge transfer resistance appearing at low frequencies,  $R_{ct0}$ , rate constant for adsorption,  $k$ , and high- and low-frequency capacity,  $C_0$  and  $C_\infty$ . Analytic expressions for all these parameters are given in ref.<sup>10</sup> and are not repeated here for the sake of conciseness.

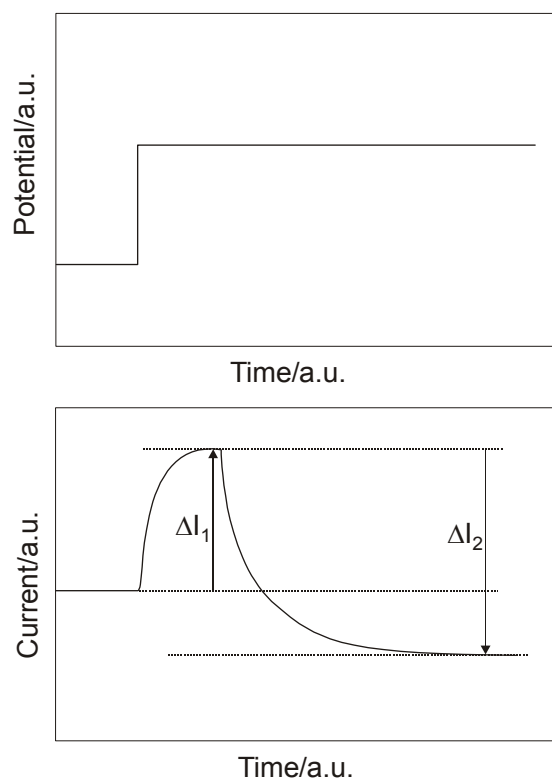


**Figure 2.** Schematic presentation of current response (below) to a potential step (above) within the active-passive transition region. For detailed explanation see text.

Let us briefly comment only on the meaning of both charge transfer resistances, because these will be the main object of present analysis.

Let us consider what happens when the potential within the active-passive transition region slightly increases in a stepwise manner (Fig. 2). At first instant, the current will also increase, in accordance to the charge transfer reaction kinetics which is usually well described by the Butler-Volmer reaction and which, at low amplitudes, simplifies to Ohm's law. In terms of the present model, this initial increase in current ( $\Delta I_1$ ) is determined by charge transfer resistance at »frozen in« adsorption,  $R_{ct\infty}$ . At a later stage, the current starts to decrease because at higher potential an additional portion of metal surface is gradually covered by adsorbing species/passive film. Finally, a new steady-state is reached with a current lower than before the excitation. The decrease of current in this second stage ( $\Delta I_2$ ) is determined by  $R_{ct0}$ . Clearly, because the current decreases while the potential is increased, the value of  $R_{ct0}$  is always negative. Also, as can be deduced from Fig.2, the absolute value of  $R_{ct0}$  is always lower than that of  $R_{ct\infty}$ .

Although the meaning of both  $R_{ct}$  values is quite straightforward, they, unfortunately, cannot be extracted from the impedance spectra, such as that in Fig.1, in a simple way. However, the sum of their inverse values:

$$\frac{1}{R_{ctsum}} = \frac{1}{R_{ct\infty}} + \frac{1}{R_{ct0}} \quad (1)$$

is quite easy to determine from impedance spectra: namely,  $R_{ctsum}$  is exactly equal to the value of impedance at frequency 0 Hz. Obviously, like  $R_{ct0}$ ,  $R_{ctsum} < 0$  (see Fig.1). Furthermore,  $R_{ctsum}$  is also equal to the inverse of the slope in I-U steady state curve at the point at which the impedance spectrum is recorded. Hence,  $R_{ctsum}$  is a parameter which connects potentiodynamic and EIS measurements in a straightforward way.

One of the specific aims of the present work was to determine the values of  $R_{ct\infty}$  and  $R_{ct0}$  at various potentials within the active-passive transition region. For this purpose, we decided to make simulations of the measured impedance spectra using the model presented above. These simulations, however, do not give a unique set of model parameters because, as mentioned, the model contains 5 parameters while the spectra containing 2 simple arcs (more precisely, semicircles) are uniquely determined already by 4 parameters. We have decided that for the purpose of the present paper, we set one of the parameters to an arbitrary and fixed value, i.e.,  $k = 1 \text{ s}^{-1}$ . In other words, we assumed that the adsorption rate constant has a typical value as observed in similar systems by other techniques<sup>10</sup> and that it does not change within the potential range of interest. In this way, we could then uniquely reproduce all measured spectra by choosing appropriate values of the other 4 model parameters.

### Experimental method

The material tested was a 13 – chromium stainless steel labelled as X20Cr13 made in Steel Works Ravne, Slovenia.

The samples with 10 mm diameter and 3 mm thickness were treated under the following conditions:

- annealed 20 minutes at 1000 °C, quenched on air
- annealed 20 minutes at 1000 °C, quenched in oil

- annealed 20 minutes at 1000 °C, quenched in oil and tempered 1 h at 250 °C.

The test samples were mechanically polished with 400, 800 and 1000 abrasive papers and fine polished with diamond pastes almost to a mirror quality. The degreasing was performed in acetone.

The measurements were made in a standard Tacussel glass cell with the specimen as a working electrode, the platinum auxiliary electrode and a saturated calomel electrode (SCE) as reference electrode. The cell was filled with 300 ml of 0.1 M H<sub>2</sub>SO<sub>4</sub> solution. The measurements were performed at room temperature. Potentiodynamic polarization curves and impedance measurements were made with a Solarton 1287 Electrochemical Interface and a 1250 Frequency response analyzer. The data were collected using CorrWare and Zplot and interpreted with CorrView and ZView softwares. All softwares were developed by Scribner Associates, Inc.

Potentiodynamic measurements were made from –1.0 V to 1.0 V vs. SCE at the scan rate 1 mV s<sup>-1</sup>.

Impedance measurements were performed in a frequency range from 60 kHz down to 0.001 Hz. The amplitude of excitation voltage was 30 mV.

EIS measurements were carried out after a 10-min polarization at a given potential. Measured potentials were chosen on the base of the classical polarization curve for X20Cr13 (Fig. 3).

### Results and discussion

Annealed X20Cr13 steel contains alloying elements, which reduce the carbon diffusion and increase corrosion resistance.

Quenching of steel prevents carbon diffusion, increases hardness, but leads to brittleness. Therefore, the steel has to be tempered before use. Tempering reduces the tension and increases the toughness, but on the other hand, causes the carbon to precipitate, leading to pitting corrosion.<sup>11</sup> Anodic polarization curves for differently heat treated steels are shown in Fig.3. Anodic currents differed with heat treating particularly in the active and active – passive transition region.

At the active peak, the current for oil – quenched steel was the highest. At potentials below this peak, the anodic currents are associated with the anodic oxidation

of steel. Higher peak currents for tempered and oil – quenched steel demonstrate that these heat treatments cause the material to corrode faster than air – quenched steel. But on the other hand, the anodic current drops more rapidly for the oil – quenched steel than for the tempered sample. To get a clearer picture about how all these phenomena are related to passivation (adsorption) and charge transfer processes, EIS measurements were performed.

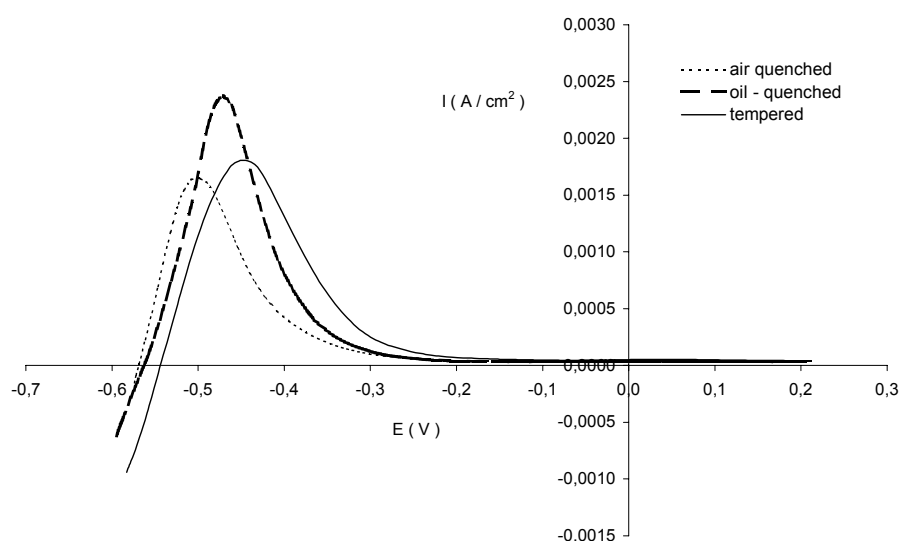


**Figure 3.** A potentiodynamic curve for X20Cr13 in 0.1 M H<sub>2</sub>SO<sub>4</sub>.

Typical measured complex - plane impedance spectra for the materials studied are presented in Fig.4. All spectra have the shapes as predicted by the model of Armstrong described above and displayed schematically in Fig.1. Of course, the model of Armstrong is only one of the many which can yield such a shape of impedance spectra. One could also use a simple equivalent circuit consisting of two RC terms, whereby the high frequency arc would represent charge transfer resistance and the low-frequency arc could correspond to adsorption. Analysis of measurements in Fig.4 using such a simple circuit, however, leads to quite unconvincing results. For example, when moving from the active dissolution peak to  $-0.33$  V/SCE (the beginning of passive state), the size of the high frequency arc (i.e., in this circuit corresponding directly to the charge transfer resistance) increases merely by a factor of 4. This, of course, cannot explain the much

larger drop in current in Fig.3 (by at least a factor of 20). Even larger discrepancy occurs, if one wants to correlate the changes in impedance and potentiodynamic curves when moving from the active peak potential to -0.4 V/SCE.

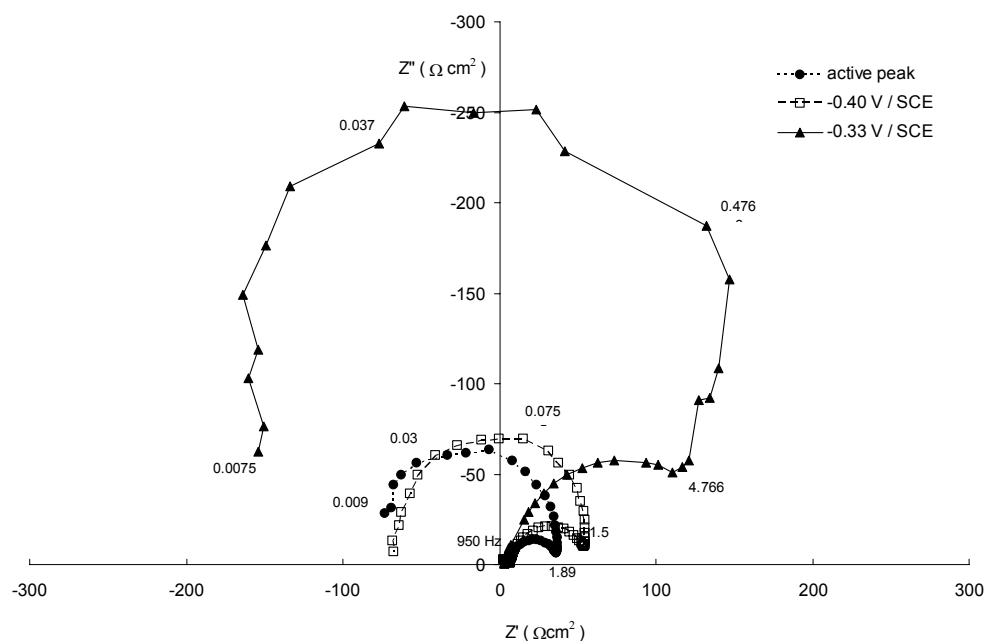


**Figure 4.** Impedance spectra for air – quenched X20Cr13 in 0.1 M H<sub>2</sub>SO<sub>4</sub> at different potentials.

Much more consistent results are obtained if one analyses the measured spectra using the model of Armstrong. Fig.5 shows simulated spectra using this model. The simulated spectra reproduce quite well the measured spectra in Fig.4. The model parameters for each spectrum are displayed in Table 1.

Interestingly, the development of the spectra with potential affects only two model parameters,  $R_{ct\infty}$  and  $R_{ct0}$  – at least at given accuracy of parameter determination.  $R_{ct\infty}$  changes from  $60 \Omega\text{cm}^{-2}$  to more than  $1300 \Omega\text{cm}^{-2}$ , which seems a reasonable result if the corresponding change of current in Fig.3 is considered. Note, however, that the actual change in  $R_{ct\infty}$  might be even larger. Namely, many simulations have shown that once the ratio  $R_{ct\infty}/|R_{ct0}|$  exceeds 10 - 15, the spectra become quite insensitive to the value of  $R_{ct\infty}$ . In other words, the spectrum at -0.33 V/SCE could be reproduced well by any value of  $R_{ct\infty}$  larger than about 1300.

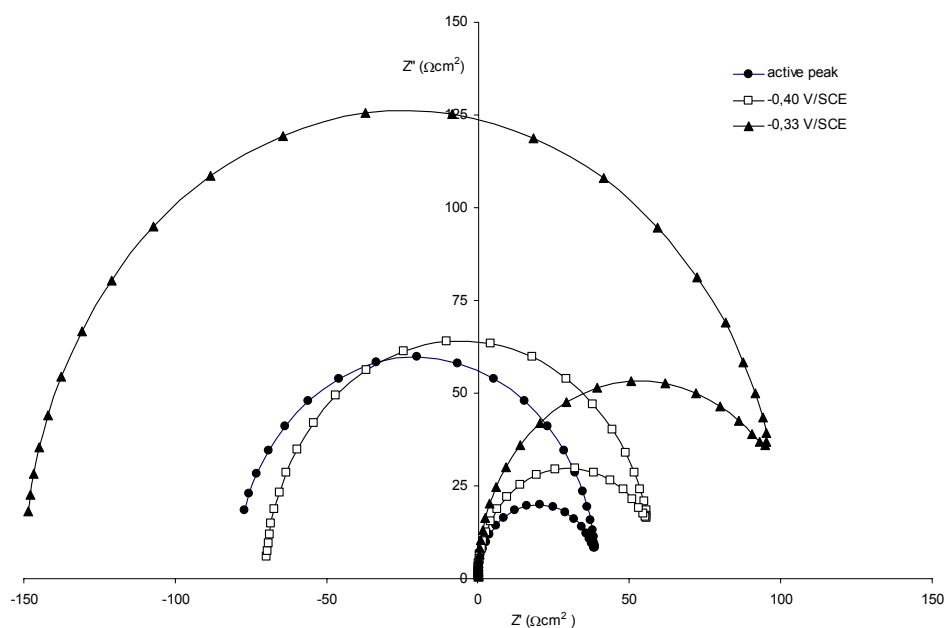


**Figure 5.** Simulated impedance spectra using the model of Armstrong.<sup>10</sup> The simulated spectra coincide well with the measured spectra in Fig.4. Some difference is observed in the spectra for the active peak. This is probably mainly due to surface inhomogeneities, especially when it gets passivated. Note, however, that this deviation of shape into extended semicircle (see Figure 4) does not affect significantly the average values of model parameters. The model parameters for the simulated graphs are shown in Table 1.

**Table 1.** Model parameter values at 3 different potentials for air-quenched steel. The value of  $k$  was selected arbitrarily,  $R_{\text{ctsum}}$  was calculated from Eq. (1). The other parameters were set to such values that the typical features of model spectra (peak frequencies, arc dimensions, frequency of high-frequency/low-frequency arc transition etc.) coincided with the measured parameters with an accuracy of  $F (1 \pm 0.1)$  where  $F$  is the value of feature under consideration.

Potential	$R_{\text{ct}\infty}/\Omega\text{cm}^2$	$R_{\text{ct}0}/\Omega\text{cm}^2$	$R_{\text{ctsum}}/\Omega\text{cm}^2$	$C_0/\mu\text{Fcm}^{-2}$	$C_\infty/\mu\text{Fcm}^{-2}$	$k/\text{s}^{-1}$
Active peak	60	-34	-80	8300	190	1.0
- 0.40 V/SCE	120	-44	-70	8300	190	1.0
- 0.33 V/SCE	>1300	<-130	-150	8300	190	1.0

It is interesting that the absolute value of  $R_{\text{ct}0}$  also increases during the passivation process. This means that the current drop  $\Delta I_2$  (see Fig.2) becomes smaller when the passivation proceeds. On the other hand, the absolute value of  $R_{\text{ctsum}}$ , which corresponds to the inverse of the slope of I-U curve, first decreases and then increases again. This variation correlates well to the fact that the I-U curve in this region exhibits an inflection.

The finding that the capacities do not change with potential in this rather small potential window is not very surprising; it is common that in interfacial electrochemistry those capacities are much less sensitive to potential than resistances.

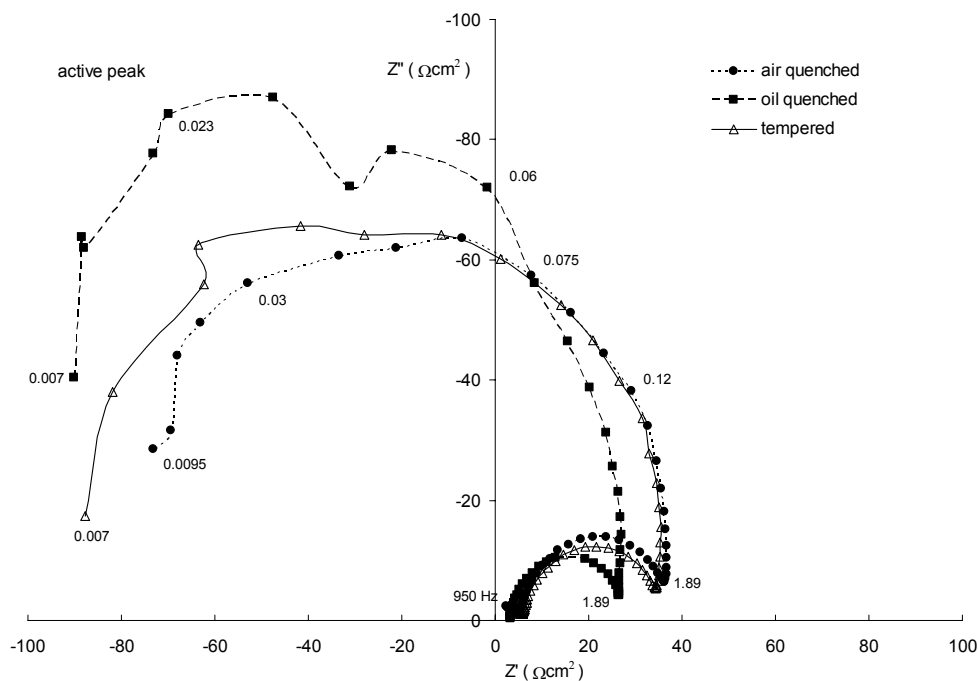


**Figure 6.** Impedance spectra for X20Cr13 in 0.1 M H<sub>2</sub>SO<sub>4</sub> at the potential of the active peak.

Figures 6-8 compare the impedance spectra of different samples at the potential of active peak, at -0.40 V/SCE and at -0.33 V/SCE, respectively.

All graphs have the same shapes which indicate that the model of Armstrong should be applicable in all cases. The values of model parameters related to charge transfer resistances are presented in Table 2. As regards  $R_{ct\infty}$ , some interesting results can be observed. At the active peak, the oil-quenched sample shows the lowest value while the air-quenched sample exhibits the highest  $R_{ct\infty}$ . This correlates well with potentiodynamic polarization data in Fig.3, i.e. the current peak is the highest for the oil-quenched and the lowest for the air-quenched sample. At -0.33 V/SCE, the  $R_{ct\infty}$  for the

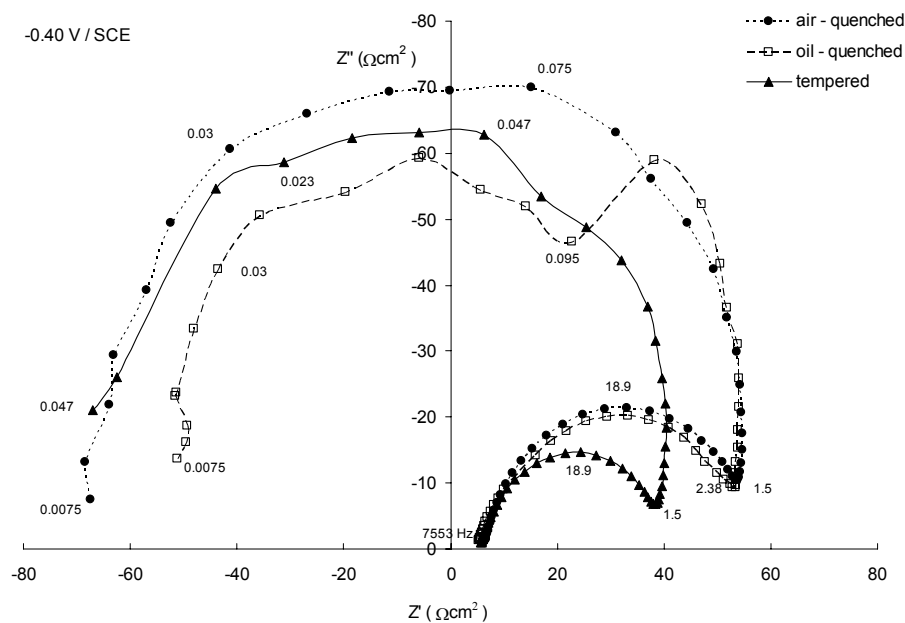


Figure 7. Impedance spectra for X20Cr13 in 0.1 M H<sub>2</sub>SO<sub>4</sub> at -0.4 V / SCE.

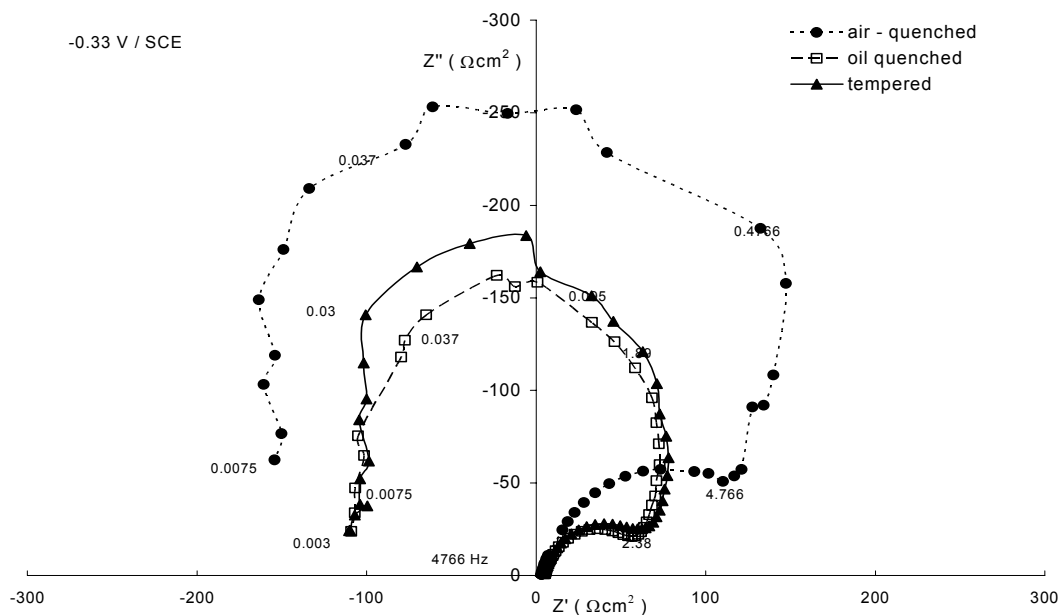


Figure 8. Impedance spectra for X20Cr13 in 0.1 M H<sub>2</sub>SO<sub>4</sub> at -0.33 V / SCE.

**Table 2.** Summary of all model-related  $R_{ct}$  values for all samples at all potentials measured. Air-qu. = air-quenched, Oil-qu.= Oil-quenched, temp. = tempered X20Cr13. The meaning of model parameters is explained in text.

Potential	Sample	$R_{ct\infty}/\Omega\text{cm}^2$	$R_{ct0}/\Omega\text{cm}^2$	$R_{ctsum}/\Omega\text{cm}^2$
Active peak	Air-qu.	60	-34	-80
	Oil-qu.	30	-23	-95
	Temp.	53	-33	-90
- 0.40 V/SCE	Air-qu.	120	-44	-70
	Oil-qu.	120	-35	-50
	Temp.	60	-32	-70
- 0.33 V/SCE	Air-qu.	>1300	<-130	-150
	Oil-qu.	300	-80	-110
	Temp.	300	-80	-110

air-quenched sample is more than 4 times larger than for the other two samples indicating the much better passivation of the former (presumably, a larger percentage of surface is covered with passive film in air-quenched sample). The model values for tempered sample at -0.40 V/SCE can be used to check the model assumption that  $R_{ctsum}$  is correlated with the slope of the corresponding steady state I-U curve (we chose this sample because at -0.4 V/SCE the slope of the potentiodynamic polarization curve is best-defined). The inverse of this slope is about 100 mV/1.5 mAcm<sup>-2</sup> which yields a resistance of 66  $\Omega\text{cm}^2$ . As seen from Table 2, the corresponding  $R_{ctsum}$  equals 70  $\Omega\text{cm}^2$ , which is not a bad agreement, especially if we take into account the fact that potentiodynamic curves are not equal to true steady state curves. In any case, it holds quite well for all measurements that the smaller the slope in the I-U curves, the higher the absolute value of  $R_{ctsum}$ .

To summarize, the air-quenched sample exhibits the largest  $R_{ct\infty}$ , at all conditions. At the active peak potential, when the surface is still almost free of adsorbates, these means that the inherent charge transfer resistance of this sample is higher than that of the other two samples. By contrast, at this potential the oil-quenched sample has much lower  $R_{ct\infty}$ , which means that it dissolves most easily among the samples. At the passive potential the air-quenched sample shows at least 4 times higher  $R_{ct\infty}$  values than the other two samples. In fact, the difference has much increased, which indicates that passivation was more successful in the case of air-quenched sample (e.g. coverage with

intermediates and products was more efficient; a smaller portion of the initial surface remained free).

As regards the oil-quenched sample, it shows the lowest  $R_{ct\infty}$  at active peak. This means that the bare surface of this material dissolves at a higher rate than in the case of the other two samples. However, at  $-0.33$  V/SCE  $R_{ct\infty}$  for this sample becomes equal to  $R_{ct\infty}$  of tempered sample. This means that this sample was protected more successfully with a passive film than the tempered one.

### References

1. F. Mansfield, W. J. Lorenz, *J. Wiley* **1991**, 581–647.
2. J.L. Dawson, M.G.S. Ferreira, *Corrosion Science* **1986**, 26, 1009–1026.
3. M. Bovine, G. Fabricius, T. Laitinen, T. Saario, *Electrochimica Acta* **1999**, 44, 4331–4343.
4. Y.J. Tan, S. Bailey, B. Kinsela, *Corrosion Science* **1996**, 38, 1545–1561.
5. I. Epelboin, M. Keddam, *J. Electrochem. Soc.* **1970**, 117, 1052–1056.
6. C. Gabrielli, F. Huet, M. Keddam, *Electrochimica Acta* **1986**, 31, 1025–1039.
7. R. Cottis, S. Turgoose, *Electrochemical impedance and noise* **1999**, NACE international, Huston, USA.
8. M. Slemnik, A. Petek, V. Doleček, *Werkst. Korros.* **1995**, 46, 13–17.
9. M. Slemnik, V. Doleček, M. Gaberšček, *Acta Chim. Slov.* **2002**, 49, 613–621.
10. R.D. Armstrong, M. Henderson, *J. Electroanal. Chem.* **1972**, 39, 81–90.
11. G. Okamoto, *Corrosion Science* **1973**, 13, 471–489.

### Povzetek

Merili smo lastnosti različno toplotno obdelanih jekel X20Cr13 v 0.1 M H<sub>2</sub>SO<sub>4</sub> s klasično potenciodinamsko metodo in impedanco. Na osnovi potenciodinamske krivulje smo izbrali konstantne napetosti, pri katerih smo izmerili impedanco: v točki aktivnega vrha, pri napetosti tik pod aktivnim vrhom in v aktivno – pasivnem področju. Pri vseh impedančnih krivuljah opazimo podobno obliko: pri visokih frekvencah dobimo lepo izražene polkroge v kompleksni ravnini, medtem ko se z zniževanjem frekvence le-ti obrnejo v nasprotno smer, katerega rezultat je t.i. negativna upornost, medtem ko se frekvenca približuje 0 Hz. Za razlago impedančnih spektrov smo uporabili model, ki ga je razvil R. D. Armstrong za elektrokemijsko reakcijo na površinah z adsorbiranim intermedijem.<sup>10</sup> Z uporabo modela na eksperimentalno dobljenih impedančnih spektrih smo lahko razložili med primeri, pri katerih je opazovana upornost prenosa naboja posledica izključno narave površine kovine in primeri, kjer je poleg tega prenos naboja določen še s stopnjo adsorbiranih intermediatov, ki dodatno pokrijejo površino kovine. Na primer, medtem ko v olju kaljeno jeklo pokaže najnižjo pripadajočo upornost prenosa naboja nepokrite površine kovine, pa na zraku kaljen vzorec pokaže največjo vrednost upornosti zaradi površine, ki jo dodatno pasivirajo intermedijati. Vsi rezultati impedančne analize se dobro skladajo z izmerjenimi potenciodinamskimi krivuljami.